Effect of boron and tungsten carbides on the properties of TiC-reinforced tool steel matrix composite produced by powder metallurgy

Slokar Benić, Ljerka; Šubić, Jadranko; Erman, Žiga

Source / Izvornik: **Archives of Metallurgy and Materials, 2020, 65, 539 - 547**

Journal article, Published version
Rad u časopisu, Objavljena verzija rada (izdavačev PDF)

https://doi.org/10.24425/amm.2020.132791

Permanent link / Trajna poveznica: https://urn.nsk.hr/urn:nbn:hr:115:176557

Arch. Metall. Mater. **65** (2020), 2, 539-547

DOI: 10.24425/amm.2020.132791

LJERKA SLOKAR BENIĆ[1*], JADRANKO ŠUBIĆ[2], ŽIGA ERMAN[3]

EFFECT OF BORON AND TUNGSTEN CARBIDES ON THE PROPERTIES OF TiC-REINFORCED TOOL STEEL MATRIX COMPOSITE PRODUCED BY POWDER METALLURGY

The influence of boron carbide and tungsten carbide on the apparent porosity, density, coercive force, hardness and microstructure of metal matrix composite of the Ferro-TiC type, is presented in this paper. The samples of investigated steel/titanium carbide composite were produced by powder metallurgy process, i.e. by powders mixing and compacting followed by sintering in the vacuum furnace. According to the results, steel/titanium carbide composite materials with addition up to 11.9 vol.% of boron carbide are interesting to detailed investigation as well as materials having more than 17.2 vol.% of tungsten carbide because these compositions show significant changes in hardness and coercive force values.

Keywords: metal matrix composite, steel/TiC composite, powder metallurgy, properties, microstructure

1. Introduction

A new class of engineering materials with toughness and machinability of tool steels, alloy steels and superalloys combined with the hardness and wear resistance of cemented tungsten carbide were recognized in iron-based composites containing titanium carbide TiC. Generally, metal matrix composites (MMCs) with steel matrix and ceramic particle reinforcements used for improving the mechanical and physical properties provide the relatively inexpensive wear-resistant materials to be produced [1-3]. Owing to its desirable properties, such as high hardness, high melting temperature, high modulus and good wettability and thermodynamic stability in molten Fe, TiC is expected to be an excellent reinforcement for Fe-based composites [4,5]. The rounded titanium carbide (TiC) particles exposed on the surface of these materials provide a combination of low coefficient of friction and hardness 30% higher than tungsten carbide (WC). This unique combination makes the Fe-based composite materials reinforced with TiC especially suitable for wear resistant applications [6]. The manufacturers of highly productive tools for plastic processing of metals as well as the manufacturers of machine parts which are subjected to surface wear have mainly two types of materials with considerably different properties available. These are tool steels, including high speed steels, and hard metals respectively. The area between these two materials is covered by a relatively new class of engineering material – tool steel reinforced by titanium carbide. This composite material known as Ferro-TiC, Ferrotitanit and TiCAlloy can be classified into the material group of cermets [7,8]. In principle, it is a hard alloy made of high chrome tool steel with a high content of carbide (~50% TiC) and produced by powder metallurgy process to obtain a high volume fraction of TiC particles in an alloy [6,9]. Namely, iron matrix composites are still favorable because of their low cost and popularity, good ductility and possibility of relatively simple treatment as well as improvement by post heat processing. TiC is one of the hardest refractory metal carbides, with a Vickers hardness of 1937-3161 HV, while Vickers hardness for WC ranges from 1835-2243 HV [10]. Hence the resultant composite is expected to possess high hardness and good wear resistance. Besides, it possesses lower density and higher thermal stability than WC [7]. Depending on the chemical composition, there is the entire spectrum of these materials having wide range of applications. Ferro-TiC shows extraordinary machinability when compared to hard metal in annealed condition and possibility of hardening to the hardness of hard metals by a simple heat treatment. Further, it shows a high resistance to surface wear, a low specific weight (depending on the chemical composition, Ferro-TiC is about 50% lighter than hard metal and 10-20% than steel), an excellent corrosion resistance and negligible dimensional changes during the heat

[1] UNIVERSITY OF ZAGREB FACULTY OF METALLURGY, ALEJA NARODNIH HEROJA 3, 44000 SISAK, CROATIA
[2] ELMECH SINTERMAK LTD., ZAGREB, CROATIA
[3] UNIVERSITY OF LJUBLJANA FACULTY OF NATURAL SCIENCES AND ENGINEERING, LJUBLJANA, SLOVENIA

* Corresponding author: slokar@simet.hr

treatment [6,8]. Therefore, it is used in hot-working, in aircrafts, and a number of other products such as: bearings, feed screws, underwater pelletizer knives, draw punches, draw rings, pill dies, P/M compaction dies, mill guide rolls, work rolls, seals, rotor fuel pumps [1,5].

New composite materials of steel matrix with TiC and WC additions respectively were developed to obtain the more resistant hard material for wear applications as cheaper alternative to cemented carbides [11]. Namely, the wear degradation of materials results in a significant economic loss [12]. Steel metal matrix composites with high volume fractions of ceramic reinforcement (50-80%) are interesting for the applications of required high hardness and wear resistance [3].

According to available literature, TiC based cermets with steel as binder were studied by Kübarsepp et al. [13-15], but there are no findings of the B_4C or WC particles effects on the microstructure and properties of metal matrix composites of Ferro-TiC type. It can be find only for aluminium alloy based composites and cemented carbides respectively [16,17]. Therefore, the goal of this work was to widespread the investigations of those carbides effects on the other system, more precisely, to determine the influence of boron and tungsten carbides on the microstructure and properties of metal matrix composite of the Ferro-TiC CM grade. A composite design using different ratios of reinforcements is important for the production of new composite materials having new enhanced properties.

2. Materials and methods

In this research, Ferro-TiC CM grade (H.C. Starck, Germany) of properties given in Tables 1 and 2 is used. Boron (B_4C, 99.5 wt.% pure) and tungsten (WC, 99.8 wt.% pure) carbides of 2 μm particle size were added to Ferro-TiC CM grade on the assumption that its properties would be improved.

TABLE 1

Chemical composition of Ferro-TiC CM grade

Component	Chemical composition	
	vol. %	wt. %
TiC	45.00	34.14
Cr	10.00	11.08
Mo	3.00	4.71
Fe	41.15	49.78
C	0.85	0.29

Three groups of samples were prepared in this investigation. The first group includes five samples of Ferro-TiC CM grade with the addition of 6.2-28.6 vol.% B_4C. Five samples in the second group contain Ferro-TiC CM grade with the addition of 1-5.6 vol.% WC, while the third group includes five samples of Ferro-TiC CM grade with the addition of 6.2-26.8 vol.% WC. In Table 3 designations, weight and volume ratios of carbides and Ferro-TiC and densities calculated according to ISO 2738:1999 are given as well.

TABLE 2

Physical-mechanical properties of Ferro-TiC CM grade [6]

Property	Value
Density	6.45 g cm^{-3}
Compressive strength	3320 MPa
Hardness (annealed)	490 HV
Hardness (hardened)	1010 HV
Coercive force	61 Oe, 4.9 kAm^{-1}
Dimensional change during the heat treatment	±0.025%

TABLE 3

Designations, weight and volume ratios of carbides and Ferro-TiC CM grade and calculated densities of investigated samples

Sample	B_4C		WC		Ferrotic CM	Calculated density
No.	wt. %	vol. %	wt. %	vol. %	wt. %	g cm^{-3}
0	—	—	—	—	100.0	6.45
1	2.5	6.2	—	—	97.5	6.21
2	5.0	11.9	—	—	95.0	5.95
3	7.5	17.2	—	—	92.5	5.77
4	10.0	22.1	—	—	90.0	5.58
5	12.5	26.8	—	—	87.5	5.40
6	—	—	2.5	1.0	97.5	6.55
7	—	—	5.0	2.1	95.0	6.65
8	—	—	7.5	3.2	92.5	6.75
9	—	—	10.0	4.4	90.0	6.85
10	—	—	12.5	5.6	87.5	6.96
11	—	—	13.8	6.2	86.2	7.02
12	—	—	24.7	11.2	75.3	7.54
13	—	—	34.4	17.2	65.6	8.08
14	—	—	40.7	22.1	59.3	8.48
15	—	—	47.0	26.8	53.0	8.91

The samples were produced by powder metallurgy process, since besides the simplicity, the raw material savings and low energy costs are ensured in this way [3,10]. The first step in the preparation of samples is mixing of components, that is powder of Ferro-TiC CM grade with boron carbides (B_4C) powder and tungsten carbide (WC) powder respectively in ratios listed in Table 3. A mass of powder mixture of each sample was 150 g. The powders were mixed in a laboratory atritor, a mixing and grinding powder machine. A hexane (0.6 dm^3) as medium was added in atritor to enhance the mixing and prevent the possible oxidation of powders. In powder metallurgy generally, the addition of lubricants can have several effects, such as: reducing frictional forces among powder particles, and between a compact and mold as well. Also, it significantly affects the flowability of the mixture consisting of iron powder and lubricant and mold release too [18]. Further, 200 g of mixing balls, 2 mm in diameter each, made from hard metal alloy type K20 (according to ISO code: 6 wt.% Co, 94 wt.% WC) were inserted in the atritor. Ball to powder mass ratio (BPR) was 1.3:1. Each sample was being mixed for 10 hours. Although the atritor is equipped with a cooling system, every half an hour the mixing was stopped

for 5 minutes to be additionally cooled. Upon the completion of mixing, hexane was removed. For that purpose, powder mixture, balls and hexane were transferred into a vessel which is sealed and connected to the liquefaction system. Then, the balls were separated from the mixture of powders using the vibrating sieve. A lubricant was added to compact the powder. After mixing and hexane removal, 3 wt.% of paraffin (T_m = 62°C) as a lubricant is added into the water heated atritor to the powder mixture to ensure its compaction. The paraffin is dissolved in special petrol. The process of paraffining is performed in the water heated atritor in order to enhance the paraffining and petrol evaporation. The obtained mixture was sieved using the laboratory sieve of 80 meshes to ensure a properly filling of tool. Then, the samples were compacted in the hydraulical press under the pressure of 220 MPa into a form of 12.5 mm in diameter tablets. The tablets were crushed and then 0.3-0.4 mm in diameter powder granules were extricated in the separator. The sieved powder mixture thus obtained was compacted using the mechanical powder press with the standard tool PV 208. The compaction pressure was 30 MPa. Green density of samples at that time was 20-22% less then density of sintered samples. All samples were deparaffined in the Balzers ROV25 vacuum furnace at 750°C. The sintering process was performed in different conditions (Table 4) in the Balzers IOV16 vacuum furnace in which argon micro leak is introduced at flow rate 100 mbar/min.

TABLE 4

Sintering conditions in Balzers IOV 16 furnace type

No.	Time/min	Temp./°C	Vacuum pressure/MPa	Argon pressure/MPa
I	15	1290	2×10^{-2}	3×10^{-2}
II	30	1380	2×10^{-2}	3×10^{-2}
III	40	1380	2×10^{-2}	3×10^{-2}
IV	40	1360	2×10^{-2}	3×10^{-2}

The samples were sintered on graphite plates. Since samples contain a high percent of iron (Table 1) which possesses a large affinity to carbon, a layer of alumina was applied in order to prevent carbon incorporation in samples during sintering. This Al_2O_3 layer was applied by plasma spraying of alumina powder on the graphite plates.

The sintered samples were metallographically prepared in three steps. First, samples were grinded by diamond plate with cooling suspension. Thereafter, fine grinding, i.e. coarse polishing of samples was performed on the rotary polishing machine using the diamond paste with diamond powder grit size 7-5 μm. Finally, samples were fine polished on a laboratory polishing machine using a diamond paste with diamond powder grit size 1-05 μm on Plexiglass plate. Before etching the samples, method for metallographic determination of apparent porosity according to ISO standard 4505:1978, was applied. This was done using the light microscope at magnification of 200× for determination of porosity of type A and 100× for determination of porosity of types B and C respectively. Type A covers pore diameters less the 10 μm, type B covers pore diameters between 10 and 25 μm, while type C covers porosity developed by the presence of free carbon. The degree of porosity is given by four numbers ranging in value from 02 to 08. The number provides a measure of pore volumes as a percentage of total volume of the sample [19]. The apparent porosity was determined by comparing the obtained micrographs with the range of photomicrographs in the above mentioned standard. The sintered density was measured by Archimedes' principle, i.e. by weighing the samples, first in the air and then in distilled water. A drop of wetting agent was added to the water to avoid air bells. The experiment was performed according to ISO 2738:1999. The density of each sample was measured five times and the average value was calculated. Coercive force was measured by coercimeter in order to determine sintering parameters effect on the structure of investigated composite material. Namely, value of coercive force can be considered as a degree of structure development which has effect on the mechanical properties [20]. The hardness of all polished samples was determined by Vickers method at load 196 N (HV20) five times for each examined material. For microscopical observations by metallographic light microscope, samples were etched in the solution of sodium hydroxide, NaOH, with potassium ferricyanide, $K_3Fe(CN)_6$.

3. Results and discussion

3.1. Apparent porosity

Metallographic determination of the presence, type and distribution of apparent porosity and uncombined carbon in polished sintered samples of the f Ferro-TiC type metal matrix composite was realized by comparing the investigated samples micrographs to standard photomicrographs. According to the applied standard, pore size is defined as the maximum dimension of the pore in the section. The apparent porosity of type A, i.e. pores up to 10 mm was assessed by scanning the surface of the samples section at a magnification of 200×. The results can be designated as A02, A04, A06 or A08 meaning that the volume fraction of pore is 0.02, 0.06, 0.2 or 0.6 vol.%. After the required comparison, the resulting porosity in the investigated samples is designated as A02 indicating that there are practically no pores up to 10 mm in samples. The apparent porosity of type B, i.e. pores within the range 10 to 25 mm was assessed by scanning the surface of the samples section at a magnification of 100×. The resulting porosity level is designated as B02 meaning that there are 140 pores per cm^2. Uncombined carbon may precipitate into clusters of carbon particles [21]. Such small elongated defects situated close together are classified as C-defects and designated as C02 indicating a negligible amount of uncombined carbon. Unlike C-defects, the pores of type A and B were mostly rounded and randomly distributed in the microstructure of investigated samples. The porosity of type A, B and C indicates a very small porosity which has no effect on density or, in the case of unsatisfactory sintering, this effect could be noticeable meaning that the material is not usable.

3.2. Density

In Figs. 1-3 the average values of experimental densities for sintered samples are shown. The square refers to calculated values of density, circle refers to sintering conditions No. I listed in Table 4, triangle refers to sintering conditions II, reverse triangle refers to sintering conditions III while rhomb refers to sintering condition IV listed in Table 4. The graphical presentation of density dependence on chemical composition and sintering temperature of samples with B_4C is given in Fig. 1, while this dependence for samples with WC is given in Figs. 2 and 3. The agreement between the experimental and calculated results, particularly for samples containing WC, can be seen.

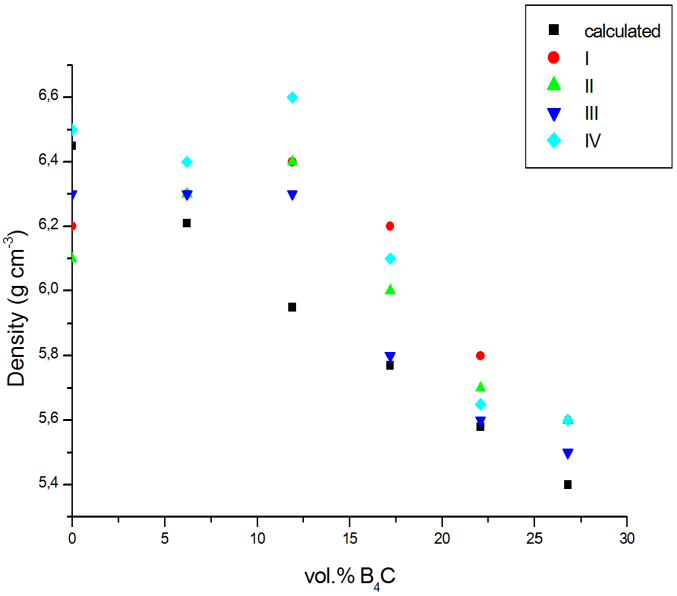

Fig. 1. Density dependence on chemical composition and sintering parameters for samples containing 6.2-26.8 vol.% B_4C (No. 1-5)

The experimental density values for samples with B_4C (Fig. 1) are in the range from 5.6 gcm^{-3} up to 6.6 gcm^{-3}. From the obtained results, it is obvious that with the increasing B_4C content above 11.9 vol.% the density of composite is decreased due to lower density of B_4C (2.52 gcm^{-3}) [22] than Ferro-TiC CM grade (6.45 gcm^{-3}). Further, it can be seen that densification increases as the sintering temperature increases for each sample meaning that the highest densification was reached at the highest sintering temperature (1380°C). The experimental result best coincides with the calculated one for samples with 17.2 and 22.1 vol.% of B_4C sintered at 1290°C for 15 min. This implies that these sintering conditions, meaning the lowest temperature and the shortest time of sintering, that resulted in densities closest to the calculated are optimal for samples with B_4C additions.

Sintered densities for Ferro-TiC samples containing lower WC concentrations are in the range from 6.3 g cm^{-3} up to 7.0 g cm^{-3} (Fig. 2). The experimental densities are the closest to the calculated values for samples sintered at the highest temperature (1380°C) for longer time (40 min). Experimental densities for Ferro-TiC samples containing higher WC concentrations (Fig. 3)

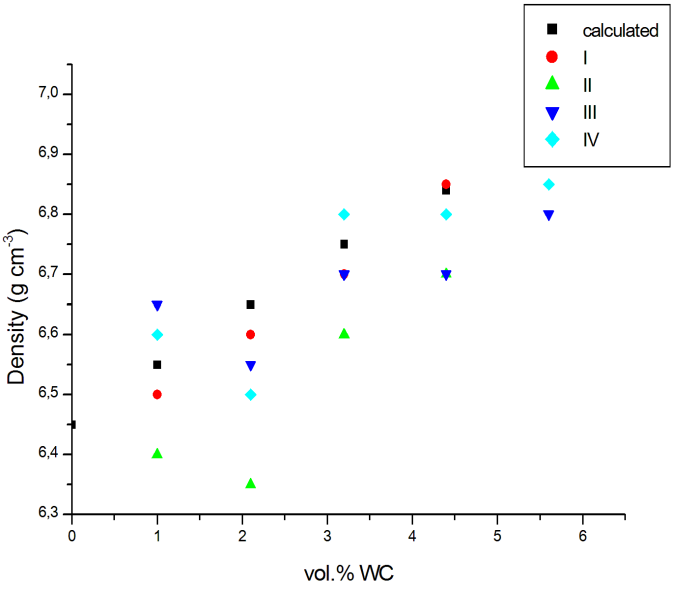

Fig. 2. Density dependence on chemical composition and sintering parameters for samples containing 1.0-5.6 vol. %WC (No. 6-10)

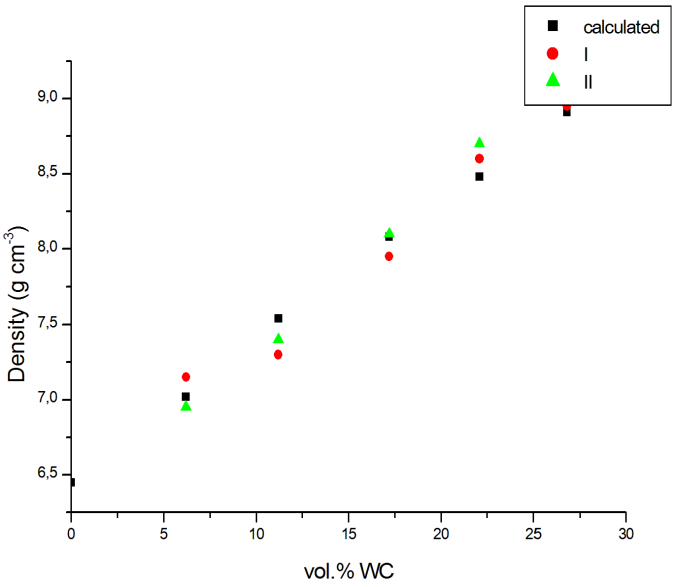

Fig. 3. Density dependence on chemical composition and sintering parameters for samples containing 6.2-26.8 vol.% WC (No. 11-15)

are in the range from 6.9 gcm^{-3} up to 9.1 gcm^{-3}. The samples with lower WC addition at lower sintering temperature show noticeable dissipation of density values than samples with higher WC addition. The reason is that the chemical composition has more significant effect on density of composite than sintering parameters.

3.3. Coercive force

The coercive force varies with sintering temperatures and indicates the structural changes that take place during sintering. It reaches a maximum at the optimum sintering temperature and decreases at higher temperatures because of grain growth. Therefore, the measurements of coercive force permit control of

sintering process. The factors that influence the coercive force are complex, varied and interactive [19]. Figs. 4-6 graphically present the coercive force dependence on chemical composition and sintering temperature. The square refers sintering conditions No. I listed in Table 4, cirle refers to sintering conditions II, triangle refers to sintering conditions III while reverse triangle refers to sintering condition IV listed in Table 4.

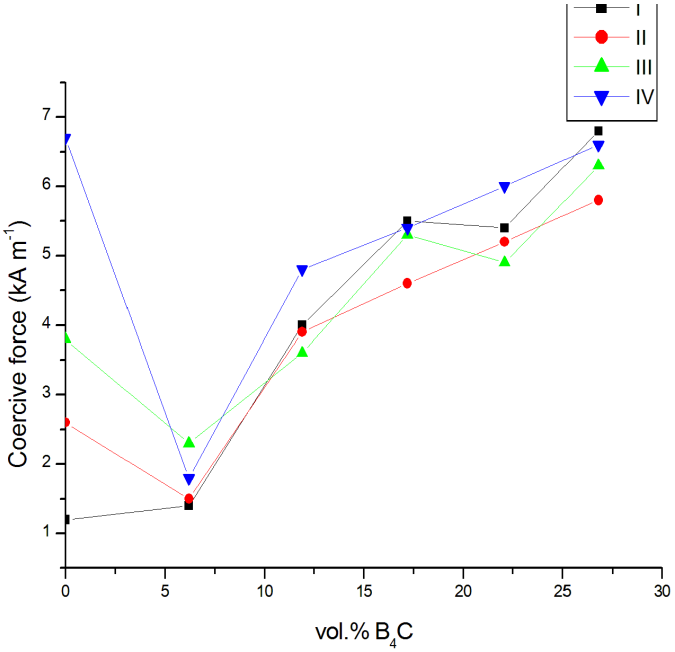

Fig. 4. Coercive force dependence on chemical composition and sintering parameters for samples containing 6.2-26.8 vol.% B_4C (No. 1-5)

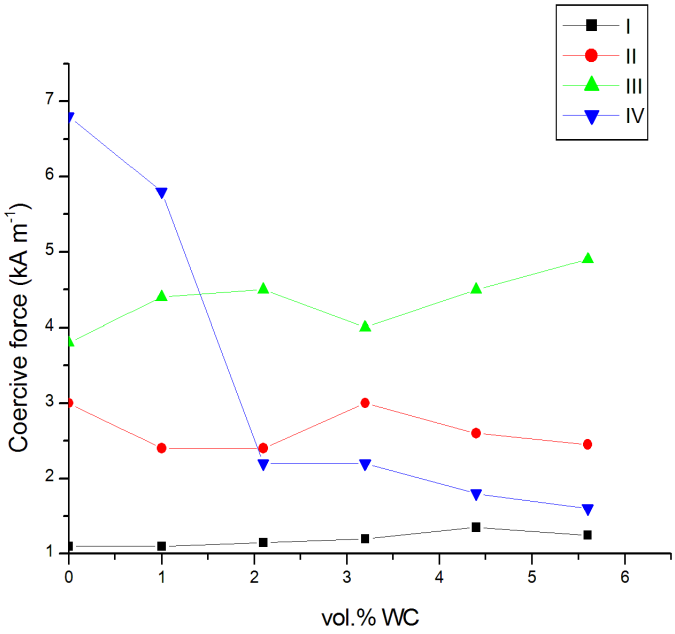

Fig. 5. Coercive force dependence on chemical composition and sintering parameters for samples containing 1.0-5.6 vol.% WC (No. 6-10)

In Fig. 4 the results for B_4C samples are shown. The values of coercive force for Ferro-TiC with B_4C are in the range from 1.2 kAm^{-1} up to 6.8 kAm^{-1}. It can be seen that coercive force

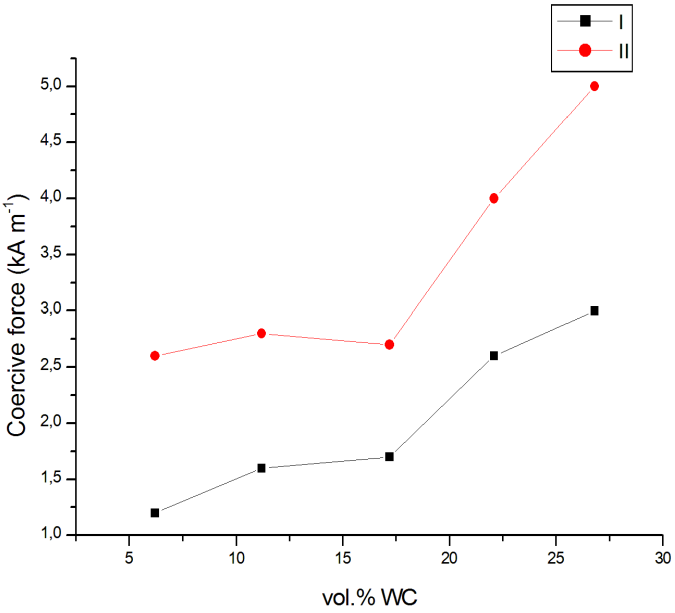

Fig. 6. Coercive force dependence on chemical composition and sintering parameters for samples containing 6.2-26.8 vol.% WC (No. 11-15)

values increase with the increasing B_4C content. The samples with addition of 17.2-26.8 vol.% B_4C reveal higher values for coercive force when compared to Ferro-TiC without B_4C addition (Table 2). Regarding sintering temperature, coercive force values are the highest for samples sintered at the highest temperature.

In Fig. 5, the small change in coercive force value for low WC concentrations is visible. Namely, the apparent stabilization of the coercive force between 1.0 and 5.6 vol.% WC can be noticed. In this group, the samples sintered at the lowest temperature (1290°C) for the lowest time (15 min) show the highest coercive force values. Overall, the values of coercive force for samples with lower WC addition are lower than Ferro-TiC CM grade without WC addition, except the samples sintered at 1380°C for 30 min. This implies that for higher coercive force achievement no high sintering temperature and long sintering time are required. For samples with 6.2 vol.% up to 26.8 vol.% of WC coercive force increases. It follows that for significant increase of coercive force values the increase in WC concentration is needed (Fig. 6). The obtained variations in coercive force values are related to matrix composition and its grain size as well as to the size of carbide inclusions.

3.4. Hardness

Hardness values of sintered samples are graphically presented on Figs. 7-9. Sintering conditions (I-IV) are listed in Table 4.

Hardness values for samples containing the B_4C are in the range from 890 HV20 up to 1450 HV20. These results are higher than hardness values for Ferro-TiC without the boron or tungsten carbide addition indicating the positive influence of boron carbide addition on the investigated composite material. In Fig. 7, which represents hardness values dependence on B_4C concentrations and sintering temperatures, the sharp rise of

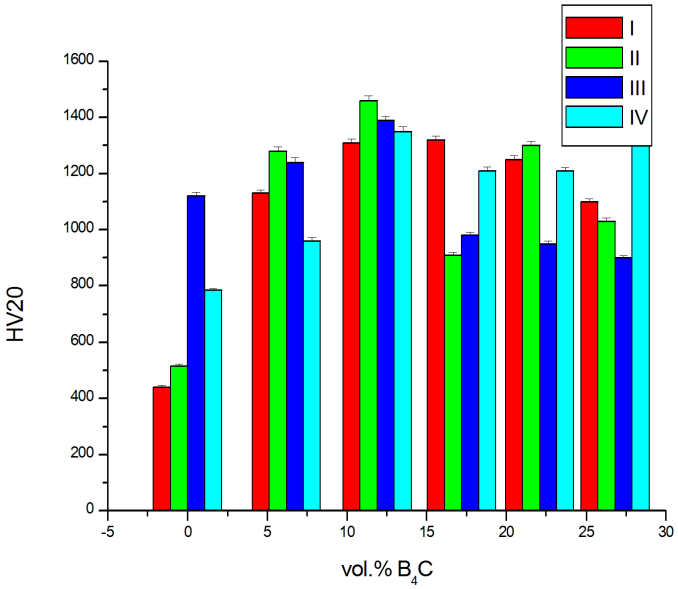

Fig. 7. Hardness dependence on chemical composition and sintering parameters for samples containing 6.2-26.8 vol.% B_4C (No. 1-5)

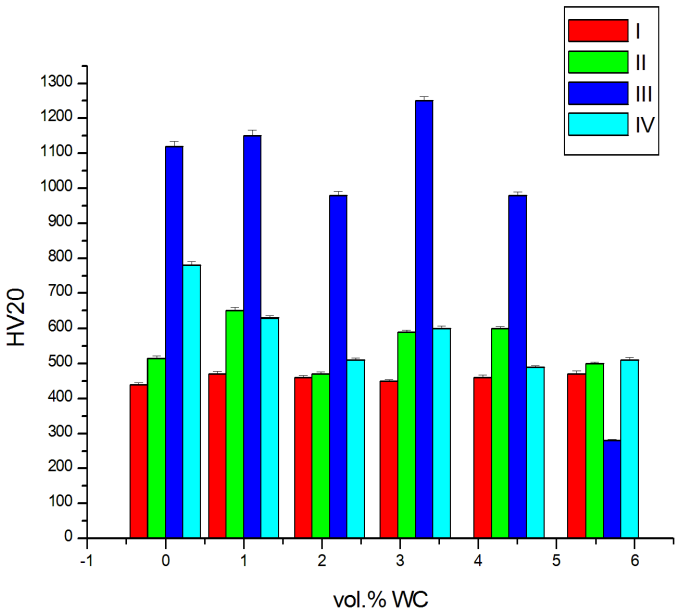

Fig. 8. Hardness dependence on chemical composition and sintering parameters for samples containing 1.0-5.6 vol.% WC (No. 6-10)

hardness as the B_4C fraction increases from 6.2 to 11.9 vol.% at all sintering temperatures can be seen. For the samples with higher B_4C volume fraction there was a decrease and variations in hardness. Blue line obtained for sintering conditions of 40 minutes and 1380°C represents regular flow of hardness curve which depends on chemical composition. Namely, up to 17.2 vol.% of B_4C obviously structure was not developed completely. After, for compositions with B_4C higher than 17.2 vol.% defect in structure occurred. Besides the composition, hardness curve depends on sintering parameters. Therefore, Fig. 7 shows sintering parameters and B_4C addition resulting in optimal hardness value. These are: sintering for 40 minutes at 1380°C with 17.2 vol.% of boron carbide.

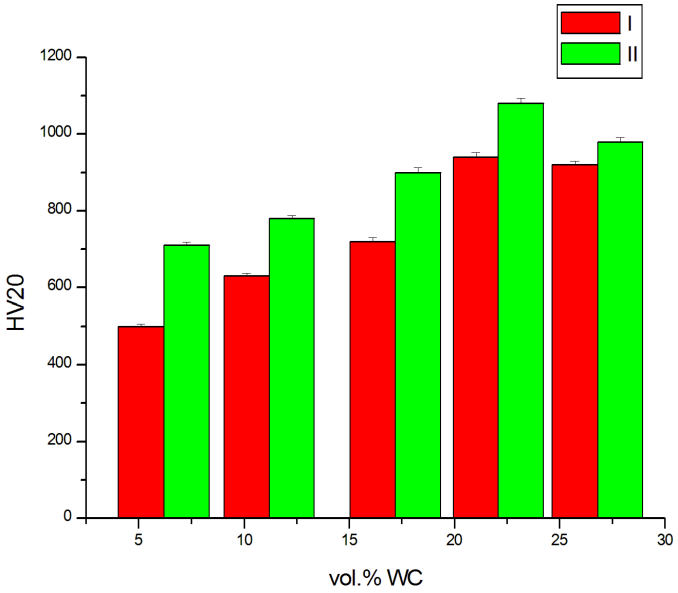

Fig. 9. Hardness dependence on chemical composition and sintering parameters for samples containing 6.2-26.8 vol.% WC (No. 11-15)

Among the samples containing lower concentrations of WC (Fig. 8), only samples sintered at 1290°C, show noticeable deviations in hardness value. The highest hardness values that are significantly higher than samples sintered at higher temperatures and longer periods are also shown. The other samples reveal approximately constant hardness, regardless of composition and sintering temperature. Obviously, in samples with 1.0-5.6 vol.% of WC, the variations in chemical composition are too small for significant changes in hardness. Hardness values in this group of samples are in the range from 250 HV20 up to 1250 HV20. Among the samples containing higher concentrations of WC (6.2-26.8 vol.%) hardness values are in the range from 500 HV20 up to 1100 HV20. It is obviously that average higher hardness values can be achieved by increasing WC content (Fig. 9). Higher hardness values for samples with 6.2-26.8 vol.% of WC at lower temperature (1360°C, Fig. 9) indicate that structure was not developed enough.

3.5. Microstructure

The investigated Ferro-TiC CM grade consists of 45 vol.% TiC with carbon martensitic tool steel matrix containing 10 vol.% Cr, 3 vol.% Mo, 0.85 vol.% C and 41.5 vol.% Fe. The microstructure of all sintered samples changes with chemical composition and significantly influences the properties of steel MMCs [6]. In Figs. 10-13 the microstructures of Ferro-TiC CM grade and samples with 11.9 vol.% B_4C, 2.1 and 11.2 vol.% of WC are shown. These samples were sintered in different conditions I-IV (Table 4).

The microstructure of samples sintered at lowest temperature (1290°C) in the shortest time (15 min) is shown in Fig. 10. The observation of microstructure of Ferro-TiC without B_4C or WC addition (Fig. 10a) revealed rounded particulate TiC rein-

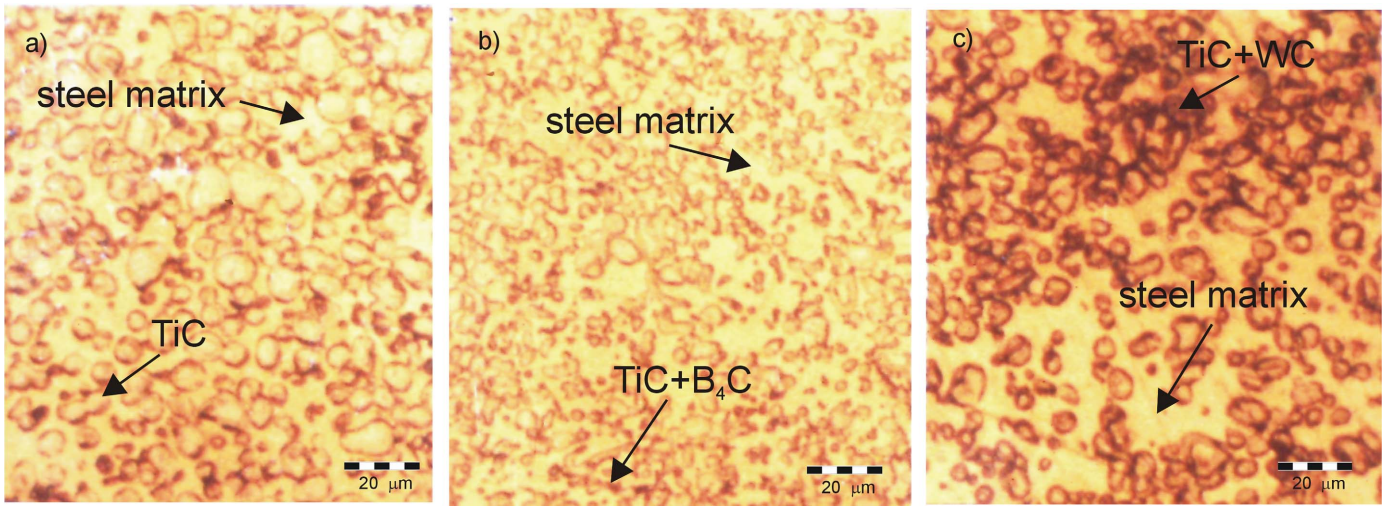

Fig. 10. Microstructure of Ferro-TiC CM composite: a) unmodified, b) with 11.9 vol. % B_4C and c) with 2.1 vol. % WC; sintering at 1290°C for 15 minutes

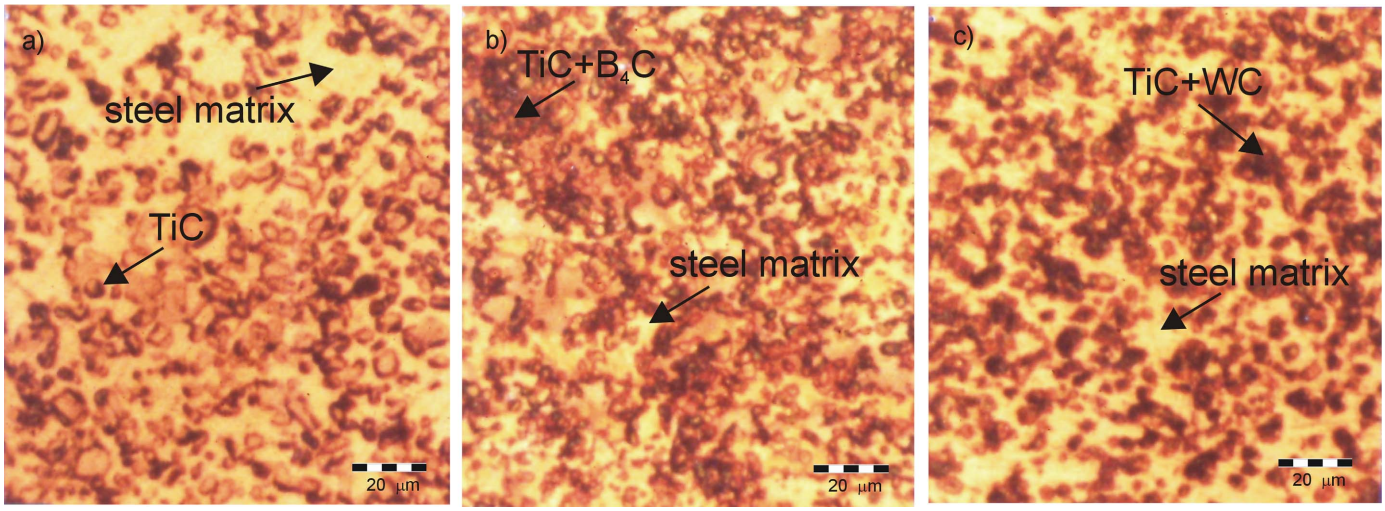

Fig. 11. Microstructure of Ferro-TiC CM composite: a) unmodified, b) with 11.9 vol.% B_4C and c) with 2.1 vol.% WC; sintering at 1380°C for 30 minutes

forcements through the steel matrix. An addition of 11.9 vol.% of boron carbide resulted in refinement of microstructure (Fig. 10b). But, addition of 2.1 vol.% tungsten carbide in steel matrix is not sufficient for refinement of microstructure (Fig. 10c). Consequently, the sample with 11.9 vol.% of B_4C showed higher hardness value than sample with 2.1 vol.% of WC.

Sintering at 1380 °C for 30 minutes resulted in microstructures shown in Fig. 11. TiC reinforcement in sample without the boron or tungsten carbides addition (Fig. 11a), carbides segregations caused by B_4C addition (Fig. 11b) and carbides due to WC addition (Fig. 11c) can be seen. The comparison of Figs. 10 and 11 shows more homogenized microstructure of sample with 2.1 vol.% addition of WC sintered at higher temperature (1380°C) for longer time (30 minutes). Namely, in given sintering conditions TiC and WC particles were more uniformly distributed in the steel matrix (Fig. 11c). In contrast, uniform distribution of the TiC and WC particles is observed after sintering at a lower temperature in the shortest time (Fig. 10a, 10b). Further, in microstructure of sample with B_4C addition higher carbides fractions can be clearly seen that cause higher values of coercive force as well as hardness when compared to sample with WC addition.

Sintering prolongation for 10 min (at the same temperature 1380ºC) resulted in microstructures shown in Fig. 12. In microstructure of Ferro-TiC CM grade without the boron or tungsten carbides addition there is no considerable change (Fig. 12a) regarding sintering conditions II. On the contrary, microstructure of sample with addition of 11.9 vol.% B_4C was refined significantly but interspersed with clusters formation (Fig. 12b). During the longer sintering period carbides in sample with 2.1 vol.% WC started to segregate (Fig. 12c) and affect the lower coercive force values as well as hardness, but higher WC addition (11.2 vol.%) resulted in finer and even carbides distribution (Fig. 12d). This prolongation time for only 10 minutes results in microstructure changes, indicating that conditionally short time is sufficient to affect the microstructure and consequently the measured properties.

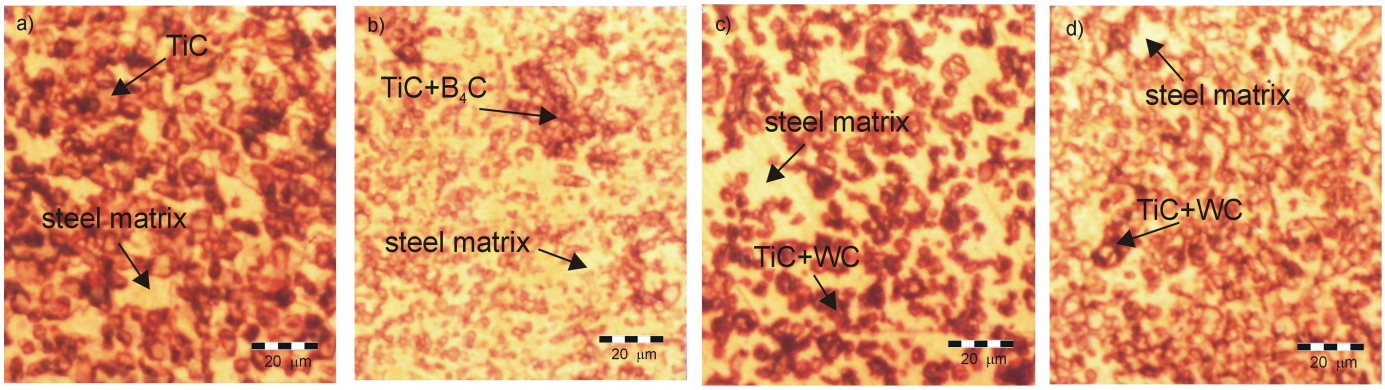

Fig. 12. Microstructure of Ferro-TiC CM composite: a) unmodified, b) with 11.9 vol. % B_4C and c) with 2.1 vol.% WC, d) with 11.2 vol.% of WC; sintering at 1380°C for 40 minutes

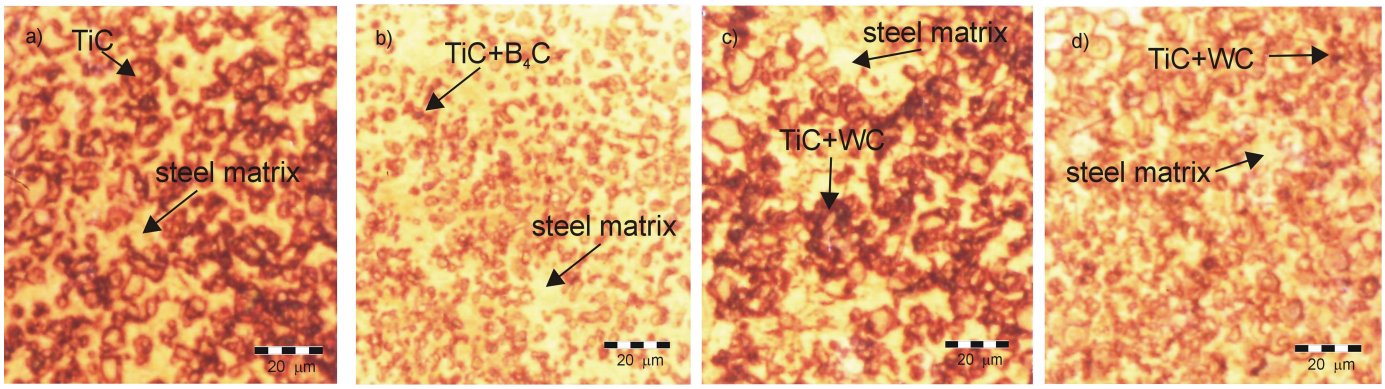

Fig. 13. Microstructure of Ferro-TiC CM composite: a) unmodified, b) with 11.9 vol. % B_4C and c) with 2.1 vol. % WC, d) with 11.2 vol.% of WC; sintering at 1360°C for 40 minutes

A slightly lower temperature (1360ºC) but the same duration (40 min) caused segregation of the TiC reinforcement in Ferro-TiC CM grade without the boron or tungsten carbides addition (Fig. 13a). In the microstructure of sample with addition of 11.9 vol.% B_4C (Fig. 12b) segregations of carbides can be seen that disappeared at higher temperature (Fig. 11b). The comparison of microstructures in Figs. 12d and 13d implies that uniform distribution of carbides with higher WC addition is favored by higher sintering temperature.

Generally, samples with addition of 11.9 vol.% of B_4C were reveal a fine microstructure, meaning that grains of titanium carbide are very small when compared to samples without the boron or tungsten carbides addition. It is particularly interesting that this appearance is independent on sintering conditions. Such a structure is just one of the reasons for the increase of hardness values and coercive force as well. The structure dominated by small carbides grains was observed in all samples containing boron carbide. This is the reason for higher coercive force values of samples with B_4C addition when compared to coarse grain microstructure of samples containing WC. Namely, fine grain size is associated with higher values of coercive force [16]. For the samples with addition of 2.1 vol.% of WC, microstructures are very similar to those for sample without carbides addition regardless of sintering conditions. This could explain a small difference in hardness and coercive force values regarding samples without carbides addition. For the samples with addition of 11.2 vol.% WC the difference can be seen in microstructures when compared to those for samples without carbides addition which corresponds to the changes in hardness and coercive force values. Finally, the examination of microstructure showed that there are no visible pores confirming the above results of porosity measurements.

4. Conclusions

In this research, the influence of boron carbide (B_4C) and tungsten carbide (WC) on the apparent porosity, density, coercive force, hardness and microstructure of metal matrix composite the Ferro-TiC CM grade is examined. From the obtained results it can be concluded as follows:

- With the increase of B_4C content in Ferro-TiC CM grade, composite density is decreased. Contrary to this, with the increase of WC content in Ferro-TiC CM grade, composite density is increased due to higher density of WC than that of composite.
- The samples with B_4C, sintered at the lowest temperature and at the shortest time showed densities closest to the calculated ones.
- Coercive force values increase with increase of B_4C content. However, equal additions of WC have a negligible effect

on the coercive force values until much higher fractions are added (>22.1 vol.% WC).

- The effect of B_4C on the Vickers hardness of Ferro-TiC CM grade depends on sintering temperature, while only the noticeable increase in WC concentration leads to the increase of hardness values.
- The examined composite exhibited higher hardness values when B_4C added to it than when WC is added.

Therefore it may be concluded that even lower additions of boron carbides favorably influence the investigated properties through a fine microstructure. However, higher concentrations of tungsten carbide are required for considerable enhancements.

These conducted researches have indicated the possible further directions of investigations. The obtained results show that the materials containing up to 11.9 vol.% of boron carbide should be investigated in detail, because those concentrations and relatively low sintering temperatures lead to significant changes in hardness and coercive force. Likewise, it is needed to conduct further investigations of these composite materials containing more than 17.2 vol.% of tungsten carbide, since the samples with those concentrations show significant changes in hardness and coercive force as properties of interest for highly productive tool production.

REFERENCES

[1] V.K. Rai, R. Srivastava, S.K. Nath, Wear. **231** (2), 265-271 (1999), DOI: 10.1016/S0043-1648(99)00127-1

[2] W. Jing, W. Yisan, Mater. Lett. **61** (22), 4393-4395 (2007), DOI: 10.1016/j.matlet.2007.02.011

[3] F. Akhtar, Can. Metall. Q. 53 (3), 253-263 (2014), DOI: 10.1179/1879139514Y.0000000135

[4] B. Li, Y. Liu, H. Cao, L. He, J. Li. Mater. Lett. **63** (23), 2010-2012 (2009), DOI: 10.1016/j.matlet.2009.06.026

[5] M. Razavi, M.S. Yaghmaee, M.R. Rahimipour, S.S: Razavi-Tousi, Int. J. Miner. Process. 94 (3-4), 97-100 (2010), DOI: 10.1016/j.minpro.2010.01.002

[6] http://www.ferro-tic.com/grade.html [cited: 2018 May 6]

[7] M. Razavi, M.R. Rahimipour, A.H. Rajabi-Zamani, Mater. Sci. Eng. A **454-455**, 144-147 (2007), DOI: 10.1016/j.msea.2006.11.035

[8] M. Foller, H. Meyer, Proceedings of the 6th International Tooling Conference: The Use of Tool Steels : Experience and Research, Vol II, Karlstad University, 1373-1389 (2002).

[9 Ö.N. Doğan, J.A. Hawk, J.H. Tylczak, Wear. **250** (1-12), 462-469 (2001), DOI: 10.1016/S0043-1648(01)00635-4

[10] Ö.N. Doğan, J.A. Hawk, J.H. Tylczak, R.D. Wilson, R.D. Govier, Wear. **225-229**, 758-779 (1999), DOI: 10.1016/S0043-1648(99)00030-7

[11] K. Liu (Ed.), Tungsten Carbide, InTechOpen (2012).

[12] I. Kovač, R. Mikuš, J. Žarnovsky, R. Drlička, J. Žitňanský, A. Výrostková, Kovove Mater. 52, 387-394 (2014), DOI: 10.4149/km 20146387

[13] M. Kolnes, A. Mere, J. Kübarsepp, M. Viljus, B. Maaten, M. Tarraste, Powder Metall. **61** (3), 197-209 (2018), DOI: 10.1080/00325899.2018.1447268

[14] H. Klaasen, J. Kübarsepp , F. Sergejev, Powder Metall. **52** (2), 111-115 (2009), DOI: 10.1179/174329008X315575

[15] H. Reshetnyak, J. Kübarsepp, Powder Metall. **41** (3), 211-216 (1998), DOI: 10.1179/pom.1998.41.3.211

[16] R. Zheng, X. Hao, Y. Yuan, Z. Wang, K. Ameyama, C. Ma, J. Alloys Compd. **576**, 291-298 (2013), DOI: 10.1016/j.jallcom.2013.04.141

[17] F. Akhtar, I.S. Humail, S.J. Askari, J. Tian, G. Shiju, Int J Refract Met Hard Mater. **25** (5-6), 405-410 (2007), DOI: 10.1016/j.ijrmhm.2006.11.005

[18] H. Suzuki, S. Nishida, T. Fujiura, Kobelco Technol Rev. **30**, 24-29 (2011).

[19] American Society for Metals, Powder Metal Technologies and Applications. ASM, (1998).

[20] R. Kieffer, F. Benesovsky, Hartmetalle, Springer, Wien (1965).

[21] A. From, R. Sandström, Int. J. Refract. Met. Hard. Mater. **14** (5-6), 405-410 (1996), DOI: 10.1016/S0263-4368(96)00041-8

[22] http://www.azom.com/article.aspx?ArticleID=75 [cited: 2018 May 11]